

Constrained spin model of phason dynamics in quasicrystals

Lisbeth D. Gronlund,* David C. Wright,[†] and James P. Sethna

Laboratory of Atomic and Solid State Physics, Clark Hall, Cornell University, Ithaca, New York 14853-2501

Daniel S. Rokhsar[‡]

IBM Thomas J. Watson Research Center, P.O. Box 218, Yorktown Heights, New York 10598

(Received 4 June 1990)

Inspired by phason dynamics in tiling models of quasicrystals, we investigate a class of constrained Ising models. Phason shifts in the Penrose tiling model of quasicrystals appear as flips of rows of tiles, known as “worms.” When worms cross one another, a hierarchy is established in which some of the worms cannot flip until others have. A complex set of constraints on worm flips is thereby introduced by the intricate pattern of worm crossings in quasicrystalline tilings. We introduce a simple model of interacting sets of one-dimensional Ising chains that mimics this set of constraints and study the possible consequences of these constraints for phason dynamics and the relaxation of phason strain in quasicrystals.

I. INTRODUCTION

Quasicrystals are a newly discovered phase of solid matter¹ that like conventional periodic crystals, exhibit long-range orientational and translational order. Unlike periodic crystals, however, quasicrystals have quasi-periodic translational order (hence the name) and may exhibit any orientational symmetry, including those forbidden in periodic crystals. (Only two-, three-, four-, and sixfold symmetries are possible for periodic structures.)

In this paper we will consider one important consequence of the unusual geometry of quasicrystals. In conventional periodic crystals in d dimensions, the free energy is invariant under a set of shifts of the phases of the Fourier amplitudes. These phase shifts correspond to translations in real space and give rise to d hydrodynamic modes which are the familiar phonon modes. In quasicrystals, the free energy is invariant under an additional set of phase shifts that correspond to local rearrangements of the atoms in real space, and that give rise to additional hydrodynamic modes called *phasons*.^{2,3} For three-dimensional icosahedral quasicrystals there are three phonon and three phason modes; for the two-dimensional pentagonal quasicrystal, there are two phonon and two phason modes.

A perfect quasicrystal would have δ -function Bragg peaks due to its long-range translational order. Only recently have several alloys been discovered that show sharp quasicrystalline diffraction peaks, indicating that long-range quasicrystalline order is possible.⁴ These quasicrystals exhibit a lattice structure that is different from quasicrystals in all previously studied materials. Measurements of Bragg peaks in all other quasicrystalline systems studied to date are broadened and shifted, indicating the presence of disorder.⁵⁻⁷ Defects occur naturally as the quasicrystal grows, giving rise to phonon and phason strains, as well as other types of defects analogous to those found in periodic crystals. An important question is whether these defects can be removed to leave a

perfectly ordered system. Diffraction studies of these samples indicate the presence of phason strain but not phonon strain.⁵⁻⁷ The interpretation is that the phonon strain (elastic distortions in the sample) can relax rapidly compared to experimental time scales, whereas phasons are either quenched in the system or have relaxation times much greater than experimental time scales. Explanations of this difference in time scales so far have assumed that a hydrodynamic description of the phason degrees of freedom is appropriate, and have explained this separation of time scales on a microscopic level.³ (Since phasons correspond to local rearrangements of atoms, the mechanism for their relaxation is diffusion, which can be a very slow process on the scale of laboratory times.)

In this paper, we will investigate an alternative model of the dynamics of the relaxation of phason strain. The real-space description of two-dimensional pentagonal quasicrystals given by a model known as the Penrose tiling^{8,9} provides a picture of the phason strain in terms of local defects that can move and annihilate each other (thus reducing the phason strain) but that are constrained in their movement.^{10,11} We are interested in how these constraints affect the diffusion of the defects and relaxation of the phason strain: Do the constraints result in phason relaxation times that are very long or infinite? Do they make the strain-free ground state inaccessible from the initial state? Do they have a hydrodynamic description at long wavelengths?

Rather than investigating the dynamics of phason relaxation in the quasicrystalline model, we present a simple Ising spin model with constraints that retains many of the features of the constraints found in the Penrose tiling model for two-dimensional pentagonal quasicrystals. (Rather different constrained spin models have been used to model glassy dynamics.¹²) Our motivation for studying this system rather than the quasicrystal tiling itself is twofold: (1) It allows us to determine the effects of the constraints on defect motion without the complications introduced by the geometry of the pentagonal quasicrys-

tal, and (2) since the behavior of the unconstrained Ising spin model is known, we can isolate the effect of the constraints.

The outline of this paper is as follows: In Sec. II, we discuss in detail the real-space description of quasicrystals, with particular emphasis on the Penrose tiling for the pentagonal quasicrystal. In Sec. III, we describe a simple spin model with three sets of interacting one-dimensional Ising chains and give the results of our calculations. We conclude, in Sec. IV, with a discussion of the implications of our results for phason relaxation in quasicrystals.

II. TILING MODEL

A tiling model provides a real-space description of quasicrystals analogous to the unit-cell descriptions of conventional crystals. In two dimensions, it is possible to produce infinitely many tilings with pentagonal symmetry and long-range quasiperiodic translational order using two rhombic tiles. These tilings can be divided into *local-isomorphism* (LI) classes,^{13,14} where two tilings are in the same LI class if and only if each finite section of one tiling can be found in the other tiling. As a consequence, tilings in the same LI class will be physically indistinguishable and, conversely, tilings in different LI classes will have different physical observables. For instance, tilings belonging to two different LI classes will have diffraction patterns given by the same set of reciprocal lattice vectors but with different Bragg-peak intensities. Thus, tilings belonging to different LI classes will have different free energies, whereas tilings in the same LI class will have the same free energy.

We will restrict our attention to one of the LI classes of two-dimensional tilings, known as the Penrose class. This LI class shares a number of special properties with three-dimensional icosahedral quasicrystals, of which there is only a single LI class. It is therefore commonly studied as a simple two-dimensional analog to the three-dimensional quasicrystal. An important property of tilings in the Penrose class is the existence of *matching rules*^{9,13} for the tiles that force an aperiodic tiling—without matching rules, the two tiles can be packed together periodically. The tiles comprising the Penrose tilings are a thick and a thin rhombus that are decorated in such a way that requiring the decorations to match on the edges of neighboring tiles constrains the way the two tiles can pack together (see Fig. 1). The matching rules therefore allow us to assign an “energy” to the system: each mismatch or violation of the matching rules is assigned a fixed energy cost.

One set of matching rules is given by the Amman line decoration of the two rhombic tiles¹³ (see Fig. 2). A Penrose tiling decorated in this way produces a grid consisting of five sets of parallel lines oriented along the five pentagonal directions (defined by the star of unit vectors pointing from the center to the vertices of a pentagon). The grid is quasiperiodic: the spacing between the lines in each set is a Fibonacci sequence of long and short spacings with a length ratio of $\tau:1$, where τ is the golden mean given by $\tau=(1+\sqrt{5})/2=1.618\dots$. This grid is

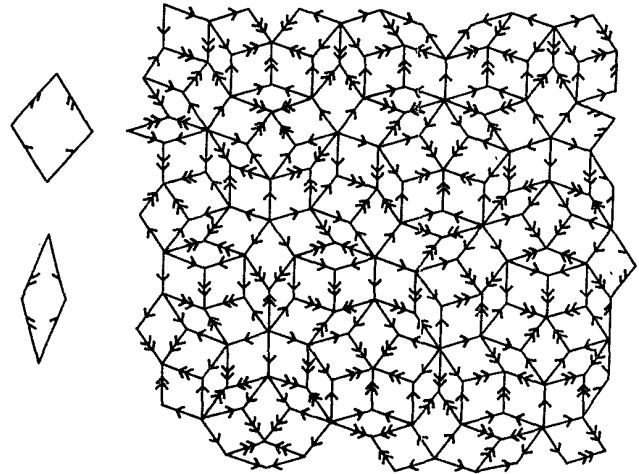


FIG. 1. The two rhombuses at the left of the figure are the two tiles used to make Penrose tiling. They have been decorated with single and double stripes on the edges. Requiring the stripes to match on the edges of two adjacent tiles so that the stripe forms a double or single arrow forces a quasiperiodic tiling. A portion of the quasiperiodic Penrose tiling is shown at the right of the figure, where the matching rules are obeyed on every edge.

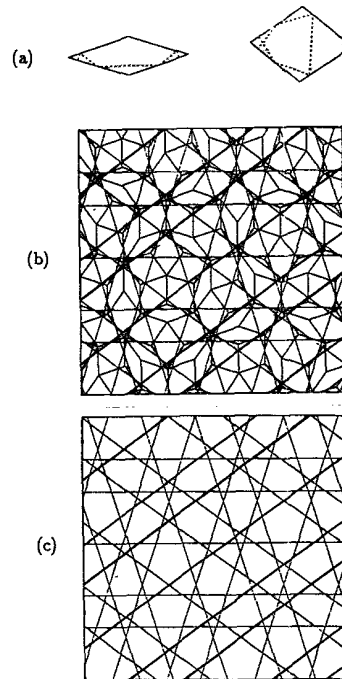


FIG. 2. (a) The two rhombic tiles with the Amman line decoration. The matching rules require that the lines be continuous across a boundary between two tiles. (b) A portion of a Penrose tiling showing the Amman decorations, which join to form five sets of parallel lines (Amman lines) oriented along the five pentagonal directions. (c) The Amman quasilattice corresponding to the Penrose tiling in (b). (Figure courtesy of J. E. S. Socolar.)

called an Amman quasilattice, and the lines are termed Amman lines. These will prove useful later in our discussion of phasons.

In the Penrose tiling, the thin and thick rhombuses combine to form two types of hexagons (see Fig. 3). One hexagon consists of two thin rhombuses and one thick rhombus, and the other consists of two thick rhombuses and one thin rhombus. These hexagons join together in straight rows, where the two hexagons are arranged in a Fibonacci sequence. Tiles arranged in such a fashion are called *worms*^{10,11} (see Fig. 3). An infinite Penrose tiling consists of infinitely many overlapping worms, each of which lie along one of the five pentagonal directions and are of infinite length. Most worms are interrupted in numerous places by the crossing of other worms.

Worms have the important property that the matching rules are identical along both edges of the worm, so that if a segment of a worm in a perfect Penrose tiling is flipped about its axis then only the matching rules at the two ends of the worm segment will be violated. There will thus be an energy cost associated with these two mismatches, which are defects in the Penrose tiling (see

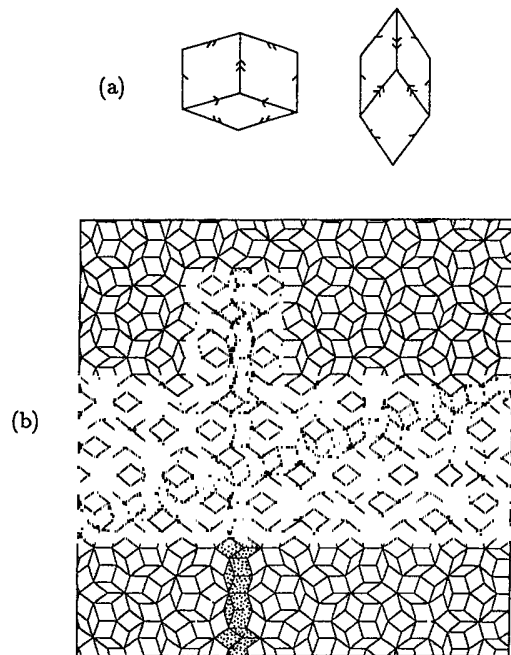


FIG. 3. (a) The two types of regular hexagons found in the Penrose tiling. Note that the top two edges of the hexagons have the same matching rule decorations as the bottom two edges, so that if either hexagon were flipped from top to bottom, the matching rules along the top and bottom edges would be unchanged. (b) In the Penrose tiling, these hexagons join together to form straight lines called worms, where the two hexagons are arranged in a Fibonacci sequence. Here, two of the worms are shaded. The nearly horizontal worm passes uninterrupted through the portion of the tiling shown; the vertical worm is interrupted by the crossing of the shaded horizontal worm and also by another (unshaded) worm at the top of the tiling. Since worms consist of a sequence of hexagons, worms also have the property that if they are flipped about their long axis, the matching rules will be unchanged along the two edges of the worm. (Figure courtesy of J. E. S. Socolar.)

Fig. 3). It is perhaps easiest to see these partial worm flips in the Amman quasilattice. With the Amman decoration of the Penrose tiling, each worm has one Amman line running along its length. Flipping a worm segment corresponds to introducing *jags* in the corresponding Amman line, as shown in Fig. 4.

A worm that is uninterrupted along its entire length can be flipped without resulting in any matching rule violations. Such worm flips result in the rearrangement of tiles with no cost in energy, and correspond to uniform phason shifts. A uniform phason shift causes a fraction of the uninterrupted worms to flip, where the number density of worms that flip is proportional to the size of the phason shift. Such worm flippings will result in new tilings in the same LI class, corresponding to different ground states of the system (since no mismatches have been introduced). There are thus an infinite number of ground states in the Penrose tiling.

The flipping of worm segments corresponds to spatially varying phason shifts, known as phason strain.^{10,11} We are interested in the question of how phason strain initially present in a Penrose tiling can relax. By flipping one of the two hexagons bordering a mismatch, the mismatch will move to the other side of the flipped hexagon (see Fig. 4). Thus, a mismatch is free to walk with no energy cost along the worm that contains it, until it comes to a point where the worm is interrupted. In this way, two mismatches in the same worm can meet and thus annihilate, or a mismatch can move off to infinity. This is the

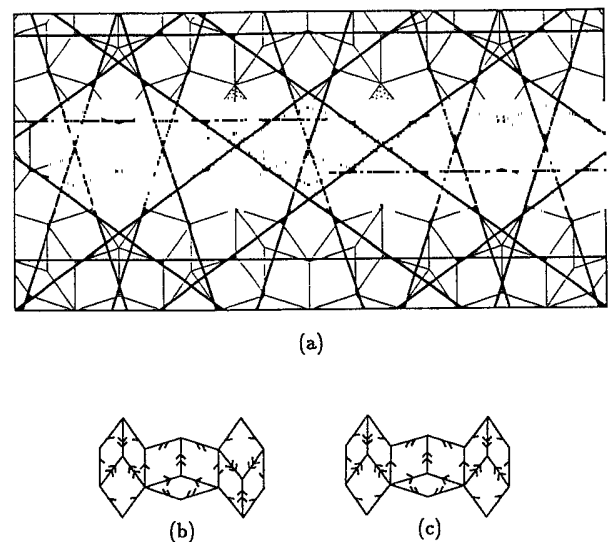


FIG. 4. (a) A portion of a Penrose tiling with the Amman line decorations shown. Each worm has an Amman line running along its length. The horizontal worm in the middle of the figure contains a matching rule violation, indicated by the broken Amman line. This break is referred to as a jag. The jag can be eliminated if the entire worm segment to the left or right of the jag is flipped. (b) The three shaded hexagons in (a) are reproduced here and shown with their matching rules. Note that there is a matching rule violation at the edge between the middle and rightmost hexagons. (c) The same worm segment as in (b), but with the rightmost hexagon flipped so that the matching rule violation is eliminated. (Figure from Ref. 10.)

mechanism for phason relaxation. Since phason strain corresponds to the flipping of worm segments, or hexagons, we will not consider tile flips other than hexagon flips. We note that it is possible to get from any space-filing tiling (including one with mismatches) to any other space-filing tiling by performing hexagon flips.

We now consider the constraints on worm flips in the Penrose tiling due to worm crossings. In the tiling, sets of tiles form two types of decagons—one with tiles arranged in a fivefold symmetric pattern, the other with tiles arranged asymmetrically. The asymmetric decagons lie at the points in the tiling at which worms cross (see Fig. 5); in fact, each such decagon can be considered to lie at the intersection of five worms, one lying along each of the five pentagonal directions. At each such intersection only two of the worms pass uninterrupted through the decagon, and segments of those two worms passing through the decagon are thus free to flip. In this way, mismatches in these two worms can walk through the decagon. We will refer to these worms as *dominant* at this decagon. The other three worms are interrupted, preventing mismatches in those worms from walking through the decagon; we will refer to them as *constrained*. The dynamics of the constraints are as follows: When the segment of one of the dominant worms passing through the decagon flips, that worm remains dominant, but the other dominant worm then becomes constrained and one of the previously constrained worms becomes dominant and is thus free to flip. (See Fig. 6 for an explicit prescription for the shift in dominance.) In this way,

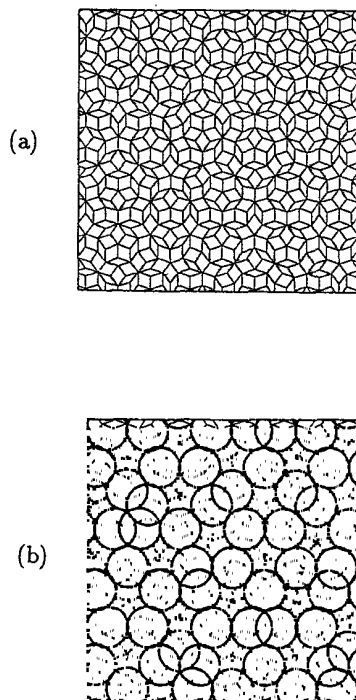


FIG. 5. (a) A section of a perfect Penrose tiling. (b) The same tiling as in (a) with the asymmetric decagons marked. Note that some of the decagons overlap one another. Each decagon is the point of intersection of five worms, one in each of the five pentagonal directions.

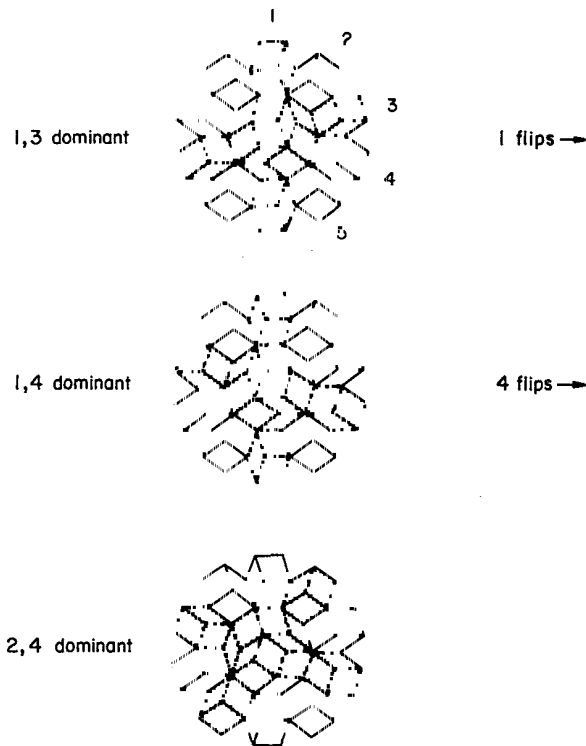


FIG. 6. A sequence of worm flips at a single decagon, which shows how the constraints shift as a result of those flips. The five worms intersecting at the decagon are labeled 1–5 and the two dominant worms in each case are shaded.

the constraints shift from one set of worms to another.

Depending on which two worms passing through a given decagon are dominant, the decagon will appear in the tiling in one of ten different orientations. In Fig. 7, we have marked the positions of all decagons with a given orientation (and its negative), i.e., those for which the two dominant worms are parallel to the same two directions. The arrangement of these decagons illustrates the high degree of order imposed on the set of constraints

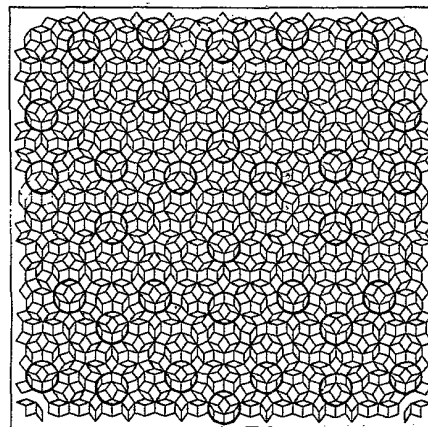


FIG. 7. All decagons for which the dominant worms are parallel to the same two directions are marked. This illustrates that the constraints are quasiperiodically ordered. If the pattern of constraints were random, the decagons marked in the figure would not have a minimum separation distance.

in the Penrose pattern by the presence of quasiperiodic order.

Consider a case where two mismatches in a worm lie on opposite sides of a decagon in which that worm is constrained. These mismatches will not be able to walk through the decagon in order to annihilate each other until the constraints in that decagon change, requiring one or more of the dominant worms to flip first. Thus, these constraints will slow down the relaxation of phason strain.

We wish to investigate the role of constraints in slowing the relaxation of phason strain. The spin model we present therefore retains the system of constraints, but ignores a number of complications in the Penrose tiling that we believe are not essential. For example, the decagons in the tiling may overlap, as is evident in Fig. 5(b), which shows a portion of a Penrose tiling with all the decagons marked. Also, worm flips can cause the decagons to vanish or shift in position.

III. THE THREE-SPIN MODEL

A. Description of the three-spin model

We abstract the qualitative features of the quasicrystal-line tiling model by representing the two states of the hexagon by an Ising spin. Since our goal is to find the simplest spin model that retains the important features of the Penrose tiling, we begin by considering a two-dimensional periodic model, where the worms are represented by three sets of one-dimensional Ising chains oriented at 120° with respect to one another.¹⁵ The chains intersect at the points of a hexagonal lattice, and there are three spins located at each of these intersections. In our model, a mismatch between two neighboring spins on a chain (i.e., antiferromagnetic alignment) corresponds to a mismatch between two neighboring tiles in a worm. In both cases, the energy cost of a mismatch is a fixed constant and the energy of the system is given by the sum of the energy costs of the individual mismatches. The spin mismatches can random walk along a chain by successively flipping spins, corresponding to the way a mismatch can diffuse by flipping tiles in the Penrose tiling. A perfect Penrose tiling with no mismatches corresponds to a spin system in a ground state. In the Penrose tiling the worms interact with each other at their intersections in the decagons. The spin chains are coupled to each other through a constraint imposed at each site to mimic the constraints in the Penrose model.

We represent this hexagonal lattice as a square lattice with the Ising chains lying in the \hat{x} , \hat{y} , and one of the two diagonal directions, say $\hat{x} + \hat{y}$ (see Fig. 8). The Hamiltonian represents the energy of three sets of independent ferromagnetic Ising chains. For a lattice of size n_x by n_y ,

$$H = H_0 - J \sum_{x=1}^{n_x} \sum_{y=1}^{n_y} [S_1(x,y)S_1(x+1,y) + S_2(x,y)S_2(x,y+1) + S_3(x,y)S_3(x+1,y+1)], \quad (1)$$

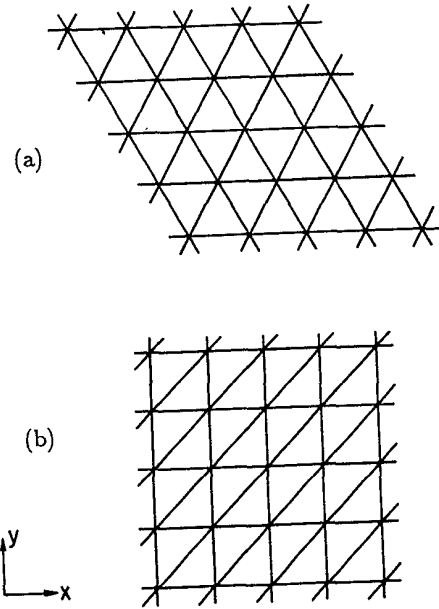


FIG. 8. (a) Each of the lines represents a one-dimensional Ising chain. The three sets of parallel lines intersect at the sites of a hexagonal lattice, and there are three spins at each site. (b) An equivalent representation of the lattice in (a), where the chains now lie in the \hat{x} , \hat{y} , and $\hat{x} + \hat{y}$ directions and the points of intersection form a square lattice.

where J is a positive constant (which we will take equal to unity) and H_0 is chosen to make the energy of the ground state zero. $S_i(x,y)$ is the value of spin i at site (x,y) , which can be ± 1 :

$$S_i(x,y) = \pm 1, \quad i = 1, 2, 3. \quad (2)$$

Periodic boundary conditions require that

$$S_i(n_x + 1, y) = S_i(1, y), \quad S_i(x, n_y + 1) = S_i(x, 1). \quad (3)$$

Since a ground state has all spins in a chain aligned (although each chain can independently have either all spins up or down), H_0 is given by

$$H_0 = 3Jn_x n_y. \quad (4)$$

While there is no energetic connection between the chains, they interact through a system of constraints. An appealing feature of this model is that the spin constraints can be set up in close parallel to the worm constraints found in the Penrose tiling. The two properties of the worm constraints, (1) that a worm that flips remains unconstrained, and (2) that the constraints change after a worm flips, uniquely determine the spin constraint and its dynamics. We define a constraint function that takes on the values $C = 1, 2, \text{ or } 3$ at each site. When $C = i$, spin i is constrained and the other two spins j and k are free to flip. If spin j now flips, it is free to flip back and the constraint switches from $C = i$ to $C = k$. For example, if we start with all spins up and $C = 1$, the following sequence of spin flips can occur: $\uparrow\uparrow\uparrow \rightarrow \uparrow\downarrow\uparrow \rightarrow \downarrow\downarrow\uparrow \rightarrow \downarrow\downarrow\downarrow$, where the three spins denote

spins 1, 2, and 3 at a given site and a bar over a spin indicates that spin is constrained. With this set of constraints, a spin on average will be free to flip $\frac{2}{3}$ of the time. This is analogous to what happens in the Penrose tiling, where the constraints shift when a worm flips, but always leave that worm free to flip back. The difference between the two models in this regard is that the decagons in the Penrose tiling always have three constrained worms whereas our spin model has only one constrained spin per site. We will discuss later the possible consequences of this difference for the dynamics of the spin model versus the Penrose tiling.

There are eight possible spin configurations at a site. The constraints limit the accessible spin configurations at each site to six of the eight; which six are accessible at a given site depends on the initial spin configuration and constraint at that site. There are four different sets of six spin and constraint configurations, in which each of the configurations is accessible from any of the other configurations in that set. (Since there are eight spin configurations and three constraint values, there will be 24 different spin and constraint configurations.) These four sets are the following:

$$\begin{array}{cccc}
 1 & 2 & 3 & 4 \\
 \bar{\uparrow}\bar{\uparrow}\bar{\uparrow} & \bar{\uparrow}\bar{\uparrow}\bar{\uparrow} & \bar{\uparrow}\bar{\uparrow}\bar{\uparrow} & \bar{\uparrow}\bar{\uparrow}\bar{\downarrow} \\
 \bar{\uparrow}\bar{\downarrow}\bar{\uparrow} & \bar{\downarrow}\bar{\uparrow}\bar{\uparrow} & \bar{\downarrow}\bar{\uparrow}\bar{\uparrow} & \bar{\downarrow}\bar{\downarrow}\bar{\downarrow} \\
 \bar{\downarrow}\bar{\downarrow}\bar{\uparrow} & \bar{\downarrow}\bar{\downarrow}\bar{\uparrow} & \bar{\downarrow}\bar{\downarrow}\bar{\downarrow} & \bar{\downarrow}\bar{\uparrow}\bar{\uparrow} \\
 \bar{\downarrow}\bar{\downarrow}\bar{\downarrow} & \bar{\downarrow}\bar{\downarrow}\bar{\downarrow} & \bar{\downarrow}\bar{\downarrow}\bar{\downarrow} & \bar{\downarrow}\bar{\uparrow}\bar{\uparrow} \\
 \bar{\downarrow}\bar{\uparrow}\bar{\downarrow} & \bar{\uparrow}\bar{\downarrow}\bar{\downarrow} & \bar{\uparrow}\bar{\downarrow}\bar{\downarrow} & \bar{\uparrow}\bar{\downarrow}\bar{\uparrow} \\
 \bar{\uparrow}\bar{\uparrow}\bar{\downarrow} & \bar{\uparrow}\bar{\uparrow}\bar{\downarrow} & \bar{\uparrow}\bar{\uparrow}\bar{\downarrow} & \bar{\uparrow}\bar{\downarrow}\bar{\downarrow}
 \end{array} \quad (5)$$

Thus, if a given site has an initial spin and constraint configuration of, say, $\bar{\downarrow}\bar{\uparrow}\bar{\uparrow}$, only the spin configurations in set 3 will be accessible at that site. Note that the system has an up-down symmetry in that if a spin configuration is accessible, so is its negative (with no change of constraint). Thus, there will always be an even number of ground states.

We now specify the dynamics of the spin system.¹⁶ In our computations, we pick a site and a spin at that site at random. If that spin is free to flip then it does so with probability

$$p = \begin{cases} 1, & \text{if } \Delta E < 0 \\ \frac{1}{2}, & \text{if } \Delta E = 0 \\ e^{-\Delta E/kT}, & \text{if } \Delta E > 0, \end{cases} \quad (6)$$

where ΔE is the change in energy due to the spin flip. (The probability of a spin flip is frequently taken to be unity for the case $\Delta E = 0$, but both choices satisfy detailed balance and will lead to the same results.) There are three possible values for ΔE : (1) If a spin is initially aligned with its two neighbors and then flips, $\Delta E = 4J$. Note that a pair of spin mismatches has thereby been created, at a cost of $2J$ each. (2) If a spin is initially aligned with one of its neighbors and not the other, $\Delta E = 0$. A spin flip of this sort moves the mismatch by one lattice spacing. (3) If a spin is initially misaligned with both of its neighbors and flips, $\Delta E = -4J$. In this

case, two spin mismatches have annihilated each other.

In a system of size $n_x \times n_y$, there are $3n_x n_y$ spins. We define one time step such that there are $3n_x n_y$ flip attempts per time step; on average, each spin in the lattice attempts to flip once per time step.

We will consider three different initial spin and constraint configurations.

(1) The first initialization we will consider has all spins ordered in a ground-state configuration and the constraints assigned randomly to each site. If this system is heated to randomize the spins and then cooled, only two ground states (the initial one and its negative) will in general be accessible. For example, if all spins are initially down, each site will be restricted to the spin and constraint configurations in either sets 1, 2, or 3 from Eq. (5) above. Since each of these sets contains the spin configurations $\bar{\uparrow}\bar{\uparrow}\bar{\uparrow}$ and $\bar{\downarrow}\bar{\downarrow}\bar{\downarrow}$, the system will be able to access the two ground states with all spins up and all spins down. While it is true that other ground states may be accessible due to a fortuitous initialization of constraints, the probability of this happening will decrease as the size of the system increases. For example, if the sites for any Ising chain in the \hat{x} direction had initial constraints of only 2's and 3's (no 1's) then the spin configurations $\bar{\downarrow}\bar{\uparrow}\bar{\uparrow}$ and $\bar{\uparrow}\bar{\downarrow}\bar{\downarrow}$ would be accessible at the sites along that chain, giving rise to four ground states: all spins up; all spins down; all spins in one \hat{x} chain up, with the remaining spins down; and all spins in one \hat{x} chain down, with the remaining spins up.

Since the spin system with this initialization has two symmetry-related ground states and the interaction between the one-dimensional Ising chains produced by the constraints effectively makes this spin system two dimensional in nature, we expect that it will be in the universality class of the two-dimensional Ising model with randomness in the bond strengths. It will therefore have a nonzero transition temperature.

(2) The second initialization we will consider has ordered spins, and constraints assigned in an ordered fashion such that there are three sublattices, each with all constraints equal to 1, 2, or 3. Traveling along a chain in each of the three directions, the constraints are set to repeat in the pattern "1, 2, 3." This initialization is intended to reflect the situation in the Penrose tiling. In that case the system has accessible ground states, and the constraints in a ground state are arranged in an ordered quasiperiodic pattern (see Fig. 7). While the pattern of constraints in the Penrose tiling is much more complicated than that in the spin model, we expect that our model retains the essential physics of the Penrose tiling.

(3) The third initialization is given by both a randomly assigned spin configuration and random constraints. In general this system will not be able to reach a ground state; spin configurations from all four sets in (5) will be found in the system, and only a very fortuitous initialization will be able to produce an ordered configuration. The probability that this will happen goes rapidly to zero as the system size increases. For this reason, this initialization does not provide a good model of the Penrose tiling, since the tiling has numerous ground states, all of which are accessible from any starting configuration.

We note that a fourth possible initialization, given by randomly assigned spins and ordered constraints, is equivalent to a system with both spins and constraints assigned randomly.

B. Results of the three-spin model

We will discuss separately the results for each of the three different initial spin and constraint configurations outlined above: (1) ordered spins and random constraints, (2) ordered spins and ordered constraints, and (3) random spins and random constraints.

1. Ordered spins and random constraints

Recall from the previous discussion in Sec. III A that initializing the system with ordered spins and random constraints leads to a system with two accessible ground states that are negatives of each other. We therefore expect that just above the transition temperature the spin configuration will contain domains of spins in the two different ground-state configurations. Domains will also be present below the transition temperature if the cooling rate is rapid enough that the system has fallen out of equilibrium. Later, we will see that systems that have been quenched to a low temperature contain such domain structures.

In order to determine the effects of the constraints on the relaxation time we compare the time evolution of the constrained system with that of an unconstrained system. The two systems relax from the same randomized spin configuration, formed by heating the original ordered state, with constraints, to a temperature of $kT=1000$ for 200 time steps in order to randomize the spins. We then remove the constraints from one of the systems, quench both the constrained and unconstrained systems to the final temperature, and measure the number of spin mismatches (which is proportional to the energy of the system) as a function of time.

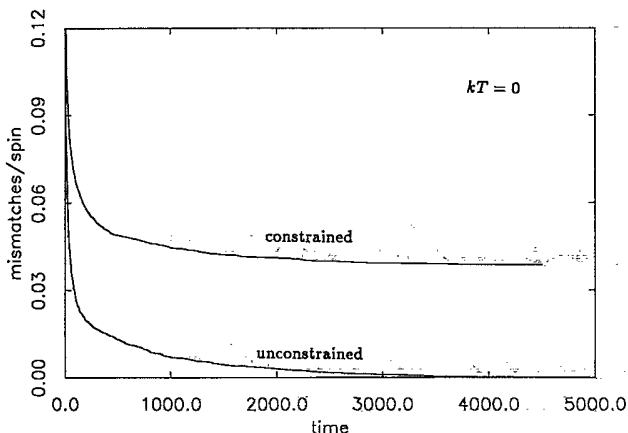


FIG. 9. The relaxation of a constrained and unconstrained system for a 100×100 lattice. Both systems were quenched to zero temperature from the same initial ground state, which was prepared by heating a configuration with ordered spins and random constraints to $kT=1000$ for 200 time steps.



FIG. 10. The graphical representation of spins and constraints in the lattice system. Up spins at a site are represented by black line segments extending in the direction of the neighbors to which the spin is coupled. The number above and to the left of the lattice point gives the value of the constraint at the site. The five configurations shown here all have spin 3 constrained, and show, from left to right, a site with all spins down, spin 1 up, spin 2 up, spin 3 up, and all spins up.

a. Quench to zero temperature. We first consider the results for a quench to zero temperature. The number of spin mismatches (normalized to the number of spins) are shown as a function of time for both the constrained and unconstrained cases in Fig. 9. The number of spin mismatches per spin is initially roughly 0.5 (at $kT=1000$) and in the first few time steps drops very rapidly as the system eliminates pairs of mismatches that are near one another. For longer times, it is apparent from the figure that the constrained system relaxes much more slowly than the unconstrained system.

We now consider the relaxation process for the constrained system in some detail. (Figure 10 explains the graphical representation used for displaying the spin configuration.) At zero temperature, no spin flips that cost energy will occur, so the system must relax without creating any pairs of mismatches. This is an important restriction. In Fig. 11 we show the spin configuration for

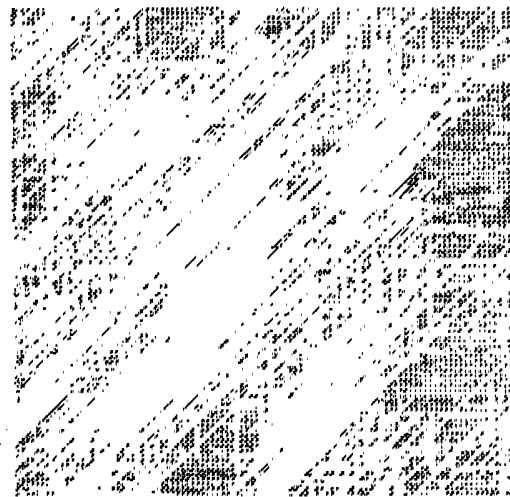


FIG. 11. The spin configuration for a constrained system 4500 time steps after quenching to $kT=0$. The lattice is 100×100 and the system has periodic boundary conditions. The initial state was produced by heating a state with random constraints and ordered spins to $kT=1000$ to randomize the spin configuration. (For a description of the graphical representation, see Fig. 10. The values of the constraints are not shown here.)

the constrained system that has been quenched to zero temperature for 4500 time steps, and in Fig. 12 we show a portion of this system with the constraints at each site indicated. Consider the up worm segment in the $\hat{x} + \hat{y}$ direction in the circle labeled A in Fig. 12. If this single spin flipped it would eliminate two spin mismatches, but it is constrained from doing so since the constraint at that site is 3. In order for the constraint to change one of the other two spins at that site must flip. However, both these spins are aligned with their neighboring spins and at zero temperature they are prevented by energetics from flipping since that would create mismatches. Thus, neither spin 1 nor spin 2 will flip until a mismatch on the worms that contain them random walks to this site. For example, the mismatch in the \hat{x} worm in the circle labeled B could random walk to site A . Spin 1 is constrained at this point, however, so this cannot occur until, for example, the mismatch at point C walked past it and changed the constraint. But this process is also constrained, e.g., by the constraint at D . Examining the section of the configuration shown, one finds that shrinking any worm segment requires a complex set of spin flips on a number of different worms in precisely the right order.

The question arises whether this spin configuration can relax to the ground state at all, or whether it tangles itself

up completely. While we have no rigorous proof, our belief is that in general the system will eventually be able to relax to one of the ground states. There are, however, exceptional configurations from which the system will not be able to relax. If the system has any single chain with no mismatches along its entire length, then no spins in this chain will flip at zero temperatures since they are all aligned. Because of the periodic boundary conditions, we will refer to such chains as *infinite*. At zero temperature, if the system contains an infinite up chain it will not be possible to get to the ground state of all down spins, and vice versa. (One must visualize not only the one up chain, but many small up segments crossing it that cannot relax due to the constraints). Thus, if the system contains both infinite up and down chains, then it will not be able to reach either ground state. This complication, however, results from the periodic boundary conditions of our system and will not occur in the thermodynamic limit. A second configuration that is unable to relax to either ground state is shown in Fig. 13. Although there are no infinite up chains in this configuration, the fact that the system cannot relax to a ground state depends on having periodic boundary conditions and chain segments of all up spins of length comparable to the size of the system. Again, the probability of having such a configuration vanishes in the thermodynamic limit.

Before considering the physically more interesting case of nonzero temperatures, it is useful to examine the relaxation process at zero temperature of a system with a region of up and down spins surrounded by a region of all down spins. Specifically, we will examine how the spin configuration in Fig. 14 can relax to the ground state with all down spins. Consider a site that contains two down chains and the end point of a chain segment of up spins (such as that labeled A in Fig. 14). Flipping the up spin shrinks the chain segment by one lattice spacing, and that spin will always be free to flip, as is evident from columns 1–3 of Eq. (5). (The initial spin configuration had all spins down, making only spin configurations in sets 1–3 accessible.) Any site that contains one down chain and the end points of two up-chain segments (such

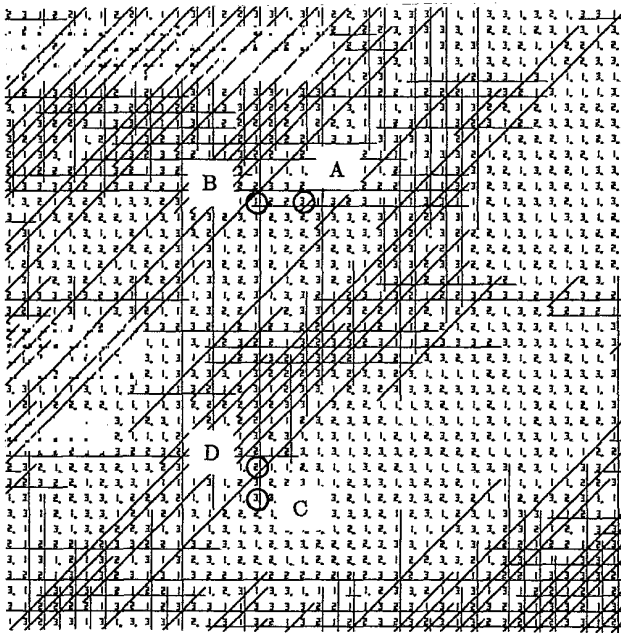


FIG. 12. A portion of the spin and constraint configuration of Fig. 11, showing the value of the constraints at each lattice site. Since the configuration is at $kT=0$, only spin flips costing no energy are allowed. In the circle at A is a pair of mismatches in the $\hat{x} + \hat{y}$ direction that cannot disappear until the constraints at that point change. The mismatch at B cannot random walk to A to change the constraint at A until the constraint at B changes. Similarly, the mismatch at C is constrained from moving to B by constraints, e.g., at D . (For a description of the graphical representation, see Fig. 10.)

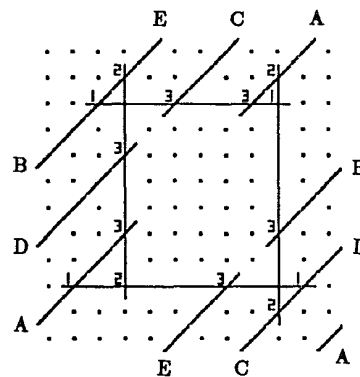


FIG. 13. A configuration that cannot relax to a uniform state at zero temperature. The numbers labeling some of the sites give the value of the constraints required at those sites to keep the system from relaxing. The letters indicate the ends of up chains that are identified by the periodic boundary conditions.

as that labeled *B* in Fig. 14) can always shrink one of the two chain segments by one lattice spacing since at least one of the two up spins will be free to flip, thus reducing the problem to that described above with one chain segment end point at that site. Similarly, if a site contains the end points of three up-chain segments (such as that labeled *C* in Fig. 14) either of the two unconstrained spins can flip, thereby reducing the problem to the previous one with two chain segment end points at that site.

By applying this process to shrink any loose chains, any configuration of one type of spins surrounded by the opposite spin can be shrunk to an isolated domain. An example of such a domain (in this case consisting of down spins surrounded by up spins) is given in Fig. 15(a). Any finite domain will have at least three convex corners, where the three spins at that site are aligned with their neighboring spins inside the domain and misaligned with their neighboring spins outside the domain. Thus, there will be no energy cost associated with flipping any of the three spins at that site, and clearly the three spins will be free to flip in succession from all down to all up. The domain in this way shrinks by one lattice site, and in the process creates new convex corners. In general this process can only occur at a corner, since anywhere else in the domain, at least one of the spins will be aligned with both of its neighbors, and energetics will prevent it from flipping. By repeating this process, two mismatches on a section of a chain forming the outer layer of the domain will eventually walk together, thereby removing that layer and shrinking the domain. Thus, eventually the domain will shrink to zero size by unraveling along the edges. Note that, although it is possible for an isolated domain to shrink to zero size at zero temperature, this will be a slow process since only the spins at the edges can flip.

The time evolution of a system with a domain at zero temperature is shown in Figs. 15(a)–15(d). Initially, there are short segments of flipped spins along the $\hat{x} + \hat{y}$ direction in the upper left and lower right corners of the domain that will disappear rapidly. By this process, a

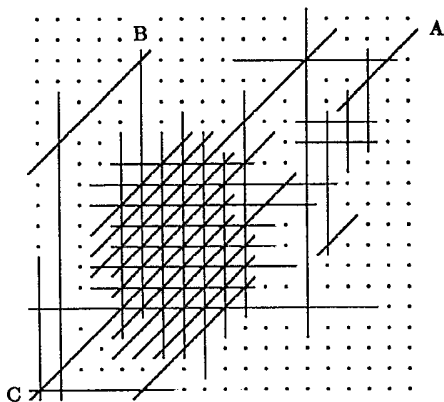


FIG. 14. A spin configuration illustrating the relaxation of mismatches at zero temperature. The spin configuration is assumed to originate from a system with all spins aligned and random constraints.

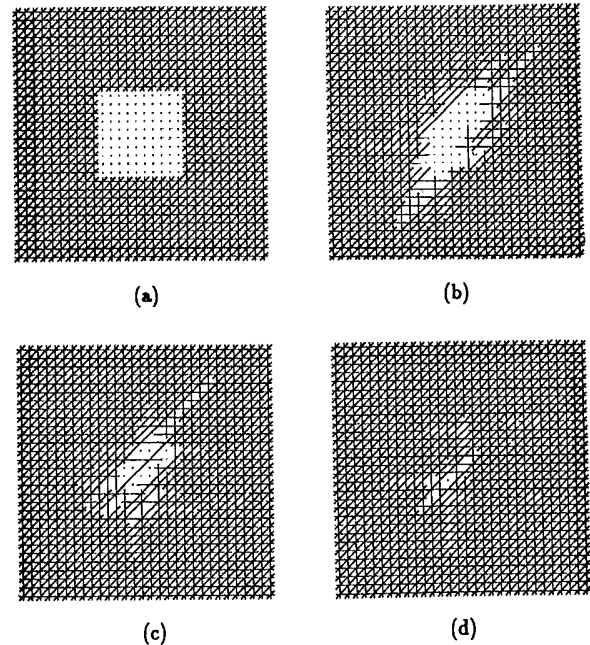


FIG. 15. The time evolution of a domain of down spins surrounded by up spins at zero temperature, shown at (a) 0, (b) 60, (c) 120, and (d) 200 time steps on a 30×30 lattice. Constraints have been assigned randomly. Notice that the short down chain segments at the upper left and lower right-hand corners of the domain in (a) disappear rapidly, producing a hexagonal shaped domain. The domain vanished by 250 time steps.

domain of arbitrary initial shape will become hexagonal, with sides parallel to the \hat{x} , \hat{y} , and $\hat{x} + \hat{y}$ directions, since any other shape would contain short worm segments. Once the short worm segments have been eliminated, the relaxation process slows down considerably since the outer layer of the domain consists of long segments of flipped spins, and it will take a long time for the mismatches at the two ends of each segment to walk together and remove that section of the outer layer of the domain. As the domain shrinks and its edges become shorter, the relaxation will speed up. We can estimate the time it takes for a domain of size L to shrink to zero by considering the time it takes for the two mismatches at the ends of a segment of flipped spins to random walk together. Since the distance between mismatches on the outer layer is of order L , this will take a time of order L^2 . Thus, in a time L^2 , the outer layer of the domain will disappear, reducing the linear dimension of the domain by two lattice spacings. This process leads to the differential equation

$$\frac{\partial L}{\partial t} \propto \frac{-1}{L^2}, \quad (7)$$

with a solution given by

$$L = (L_0^3 - ct)^{1/3}, \quad (8)$$

where c is a constant that depends on the random-walk velocity. Thus, the time it takes for a domain of size L_0 to shrink to zero scales as L_0^3 . For an isolated domain,

the number of spin mismatches is twice the length of the perimeter, so the number of mismatches also decreases as (8) (see Fig. 18).

b. Quenches to nonzero temperatures. We now consider the relaxation of constrained systems after quenching to nonzero temperatures. In this case, there will be a finite probability $e^{-4/kT}$ of creating a pair of spin mismatches by flipping a spin initially aligned with both its neighbors. This will always enable the system to untangle itself and ultimately relax to a ground state, which will contain a nonzero equilibrium number of spin mismatches produced by thermal fluctuations. We expect that the equilibrium number of mismatches for the constrained system will be less than that for the unconstrained system because the constraints will reduce the thermal fluctuations, thereby lowering the rate of creation of mismatch pairs.

During the relaxation process, we expect that the system will separate into domains. The small domains will unravel or be incorporated into other domains. Eventually, the system will contain only a small number of large domains, and at that point the relaxation process will be slowed because of the dynamics of domain relaxation discussed above.

For quenches to a temperature of $kT=0.2$, the curves showing the number of spin mismatches as a function of time for the constrained and unconstrained systems are found to be indistinguishable from the corresponding zero-temperature curves. This is expected since at $kT=0.2$, the probability of flipping a single unconstrained spin and creating a mismatch pair is $e^{-20}=2\times 10^{-9}$. A system of 100×100 lattice sites contains 30 000 spins. For the observed mismatch density of roughly 0.1, most of these spins are aligned with both their neighbors so that a spin flip would create a mismatch pair. Since a given spin is unconstrained $\frac{2}{3}$ of the time, the probability of creating a mismatch pair anywhere in the lattice is 4×10^{-5} , or once in every 3×10^4 time steps. Thus, any difference between the dynamics at zero temperature and at $kT=0.2$ will be apparent only at very long times.

The number of mismatches for an unconstrained and two constrained systems is plotted as a function of time for a quench to a temperature of $kT=0.4$ in Fig. 16. This graph shows that the constrained system relaxes faster than in the zero-temperature quench, but still very slowly compared to the unconstrained system. The unconstrained system has relaxed to its equilibrium value by 2500 time steps. We show here curves from two constrained systems to illustrate the variation in behavior that is seen at this temperature.

Figure 17(a) shows the spin configuration corresponding to the lower of the constrained curves after 4500 time steps. This picture is quite different from the comparable one for the quench to zero temperature after the same number of time steps, which is shown in Fig. 11; the zero-temperature quench has essentially stopped changing and has no ordered regions that are the size of the system. The spin configuration for this $kT=0.4$ quench after 6500 and 9500 time steps are shown in Figs. 17(b) and 17(c). For times greater than 10 000, the

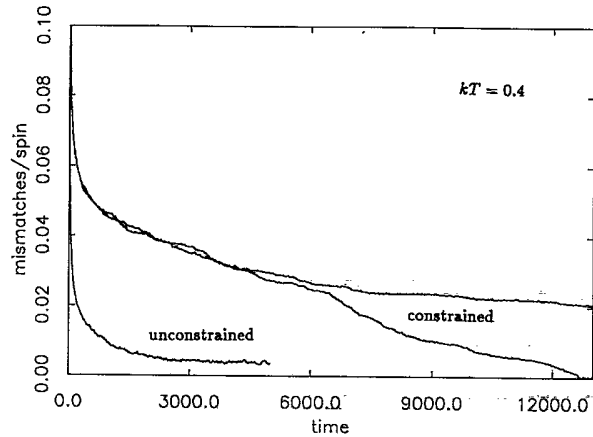


FIG. 16. The relaxation of an unconstrained and two constrained systems for a 100×100 lattice. The systems were quenched to $kT=0.4$ from initial states produced by heating samples with ordered spins and random constraints at $kT=1000$ for 200 time steps. The two constrained curves show the effects of different initial configurations on the long-time behavior of the system.

configuration contains a single domain of up spins which is unraveling, and the time dependence of the number of spin mismatches should be given by Eq. (8). In Fig. 18, we plot the cube of the number of mismatches versus the time; this curve should be a straight line if Eq. (8) holds. For times greater than 10 000, this curve indeed shows the expected linear behavior.

Note that, as expected, the constrained system has an equilibrium value less than that for the unconstrained system since the constraints reduce the thermal fluctuations.

The spin configuration corresponding to the higher of the two constrained curves at 11 000 time steps is shown in Fig. 19. In contrast to Fig. 17, this configuration shows several large domains and little else; the relaxation of this system is therefore expected to be quite slow. The large variation in the behavior of these two constrained systems can be understood in terms of the probability of creating pairs of mismatches at $kT=0.4$. At this temperature, the probability of any one spin flipping and creating a mismatch pair is $e^{-10}=4.5\times 10^{-5}$. Following the same logic outlined above, this system will create a mismatch pair somewhere in the lattice once every time step, on average. This rate is apparently large enough to allow the initial configuration to relax, in contrast to the situation at $kT=0$ and 0.2, but is small enough that the dynamics is strongly affected by the details of the initial spin and constraint configuration when the system is quenched. In the first case above, no large domains were nucleated and the relaxation could proceed rapidly. In the second case, the initial configuration led to the formation of large domains, which will relax slowly. At higher temperatures, the thermal production of mismatches appears to be sufficiently large that the relaxation process is not as sensitive to the details of the initial configuration.

The relaxation of a constrained system is compared to that of an unconstrained system for quenches to tempera-

tures of $kT=0.6, 0.8,$ and 1.0 in Figs. 20–22. Note that in all cases, the equilibrium value of mismatches in the constrained system lies below that of the unconstrained system, as was discussed above. For comparison, the number of mismatches as a function of time for the constrained quenches to temperatures of $kT=0.4, 0.6, 0.8,$ and 1.0 are plotted on the same graph in Fig. 23.

There will be roughly 25 mismatch pairs created per time step at $kT=0.6$ and 120 for $kT=0.8$. For both

temperatures, the spin configuration corresponding to the plots in Fig. 23 eventually evolves to a configuration containing one large isolated domain. As discussed above, the relaxation of a domain of this size will be very slow.

The spin configuration for the constrained system quenched to $kT=1.0$ is shown at 4500 time steps in Fig. 24. At this temperature, thermal fluctuations are frequent enough to change the character of the domains in the system. In addition to a considerable amount of

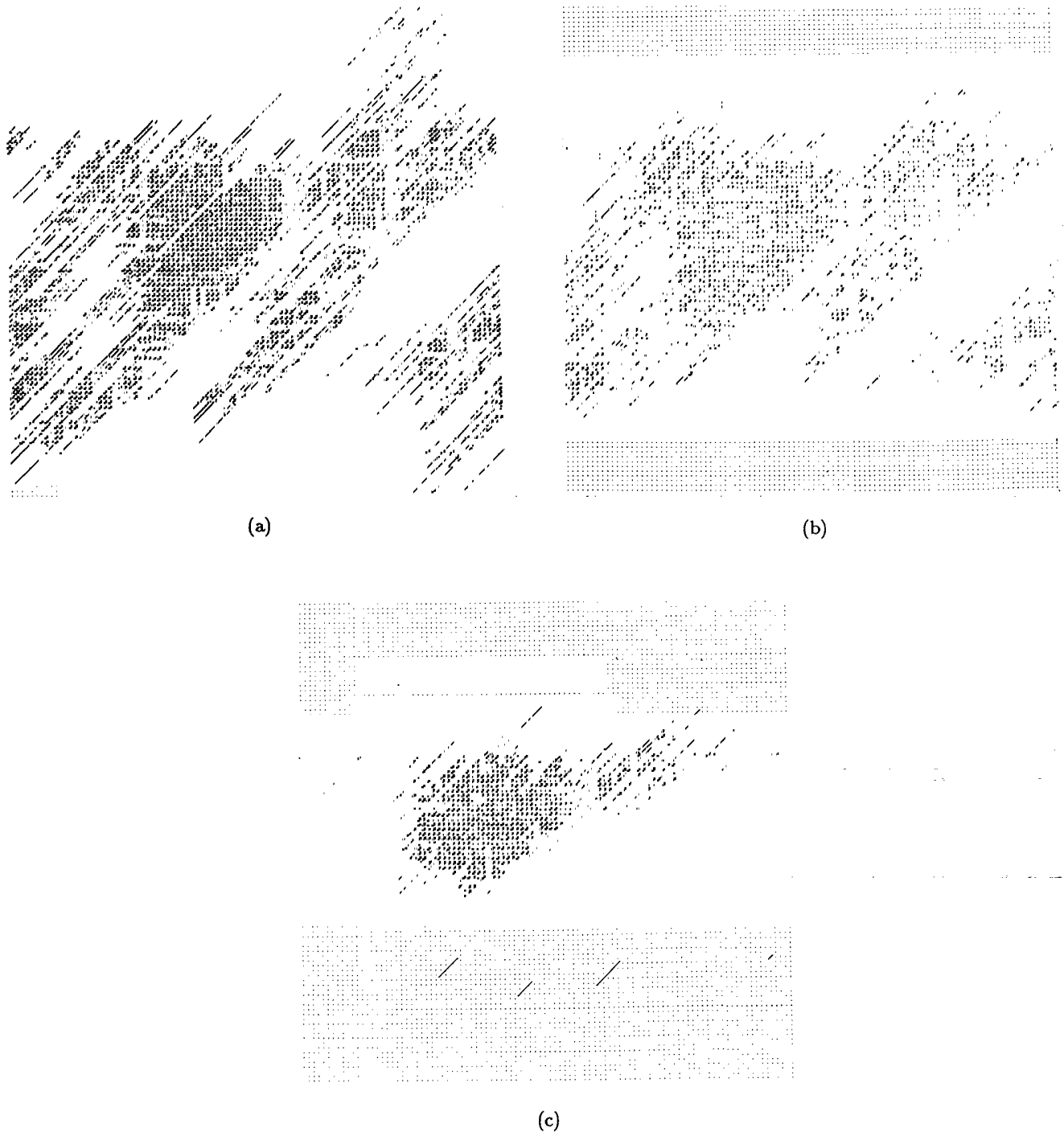


FIG. 17. The spin configuration for the lower of the constrained curves at $kT=0.4$ in Fig. 16 is shown at (a) 4500, (b) 6500, and (c) 9500 time steps. The black domain disappeared at about 12 600 time steps.

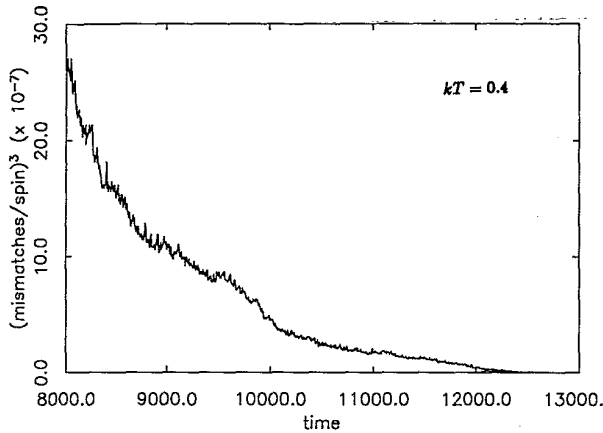


FIG. 18. A plot of the cube of the number of mismatches vs time for the lower constrained curves in Fig. 16. For times greater than about 10 000, this shows the linear behavior expected for a vanishing domain.

background thermal excitations, the figure shows a ragged domain that has broken into small regions and will therefore disappear rapidly. On the other hand, the temperature is still clearly below the critical point: the system has a large net magnetization down.

2. Ordered spins and ordered constraints

The initial configuration of ordered spins and constraints that we use in our computations is shown in Fig. 25. This initial state has all spins down and the constraint repeats in the pattern "1,2,3" in each of the three chain directions.

The ground states of this system will have the periodicity of the constraints and will therefore repeat in 3×3

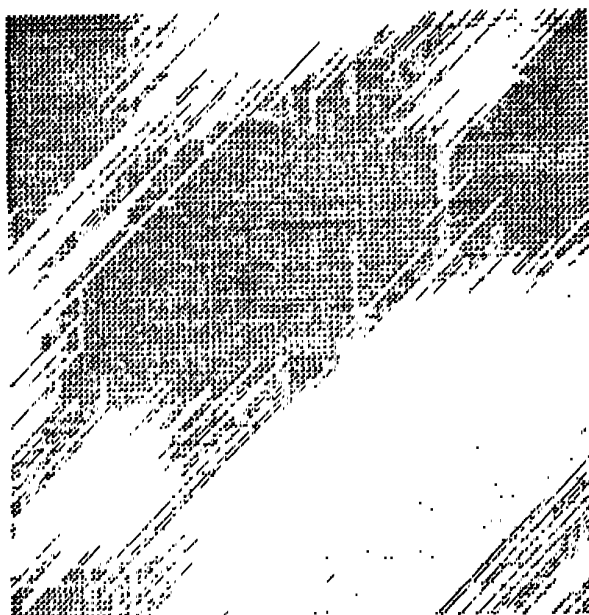


FIG. 19. The spin configuration corresponding to the higher of the constrained curves in Fig. 16, shown at 11 000 time steps.

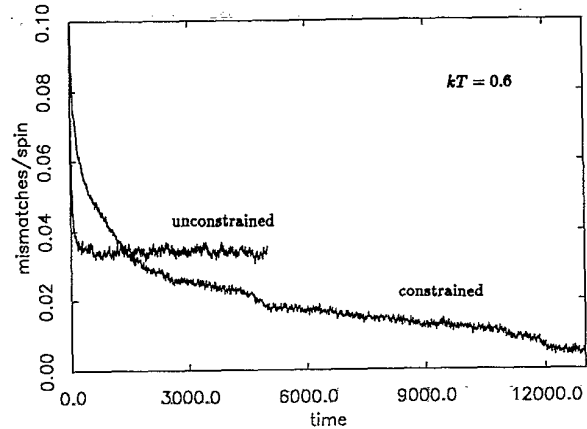


FIG. 20. The relaxation of a constrained and unconstrained system for a 100×100 lattice. The systems were quenched to $kT=0.6$ from the same initial state, produced by heating a system with ordered spins and random constraints to $kT=1000$ for 200 time steps. After 12 000 time steps, the constrained system has relaxed to its equilibrium density of mismatches.

unit cells. We can determine these ground states by considering a 3×3 lattice initialized with ordered spins and constraints, and enumerating the different possible spin configurations for each of the nine sites that produce no spin mismatches and are compatible with the constraints and periodic boundary conditions. This procedure results in seven possible spin configurations and their negatives—for a total of 14 ground states. In addition to the two ground states with all spins up and all spins down, there are two sets containing six ground states that are translations and negatives of each other. These 12 are depicted in Figs. 26(a) and 26(b).

We also considered the possibility that there could be ground states with a periodicity of 6×6 lattice sites or larger. Because of the larger number of sites, the procedure outlined above for the case of 3×3 periodicity is not easily repeated for a 6×6 lattice. However, in re-

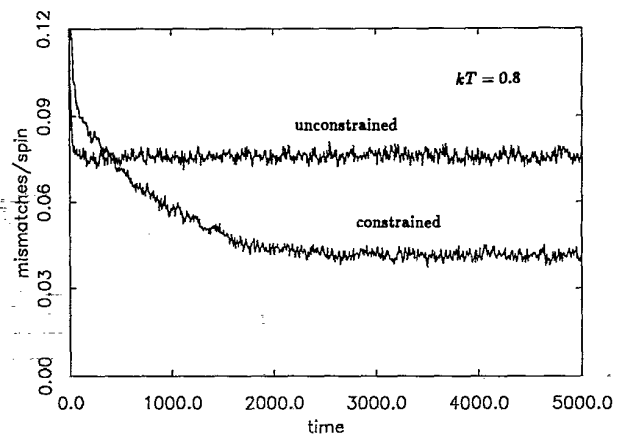


FIG. 21. The relaxation of a constrained and unconstrained system for a 100×100 lattice. Both systems were quenched to $kT=0.8$ from the same initial state, produced by heating a system with ordered spins and random constraints to $kT=1000$ for 200 time steps. After about 2000 time steps the constrained system contains one large domain that is slowly unraveling.

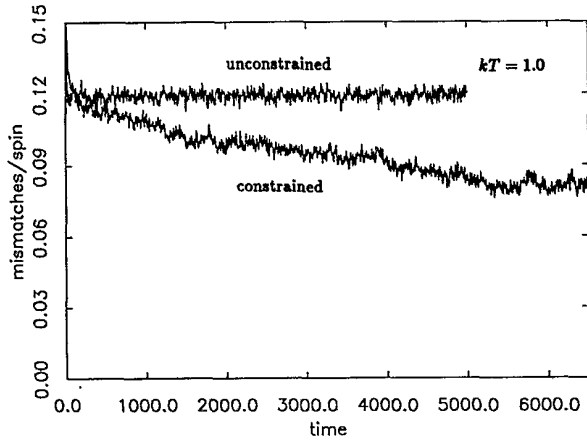


FIG. 22. The relaxation of a constrained and unconstrained system for a 100×100 lattice. Both systems were quenched to $kT = 1.0$ from the same initial state, produced by heating a system with ordered spins and random constraints to $kT = 1000$ for 200 time steps. The constrained system has relaxed to its equilibrium density of mismatches by 5000 time steps.

peated quenches of systems of size 99×99 , the only zero-energy domains we found were one of the 14 ground-state configurations with 3×3 periodicity. Thus, we believe that the 14 ground states described above are all the ground states accessible to the system.

When two different phases border each other, there will be spin mismatches along the interface, giving rise to a *boundary energy*. We now examine the boundary energies of two given domains. Since the ground states have a 3×3 periodicity, it will be useful to express the boundary energies in terms of the number of spin mismatches per three lattice constants of interface. Locally, the boundary always lies parallel to one set of chains, and the possible spin mismatches between the two domains will lie in chains in the other two directions, i.e., if the boundary is parallel to the \hat{x} direction, spin mismatches can occur in

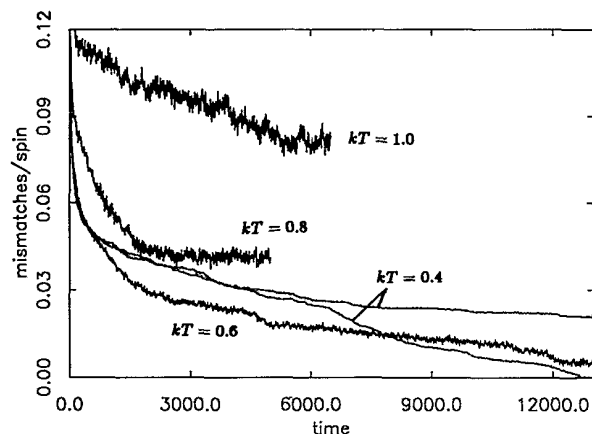


FIG. 23. A comparison of the curves for the constrained systems from Figs. 16, 20, 21, and 22.

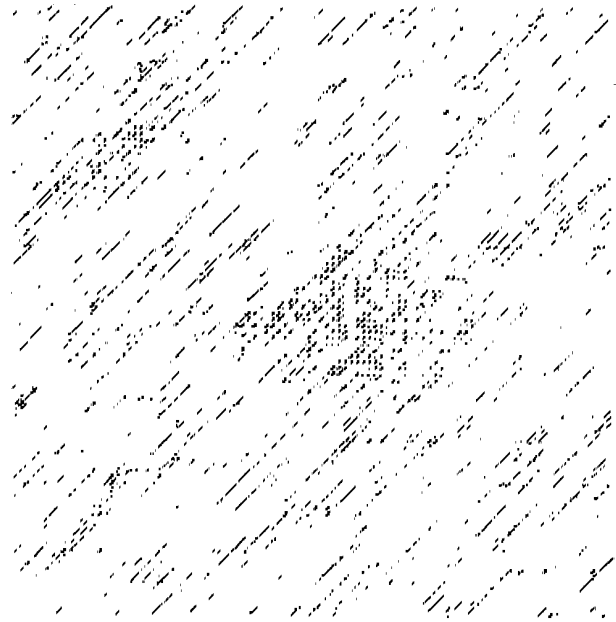


FIG. 24. The spin configuration at 4500 time steps for the constrained system plotted in Fig. 22, which was quenched to $kT = 1.0$.

the \hat{y} and $\hat{x} + \hat{y}$ chains. Thus, there will be a maximum of six mismatches per three lattice constants of interface. A boundary between two patterns that are inverses of each other will have the highest density of mismatches: six. The other two possible mismatch densities are four and two. Thus, some domains will be better matched than others (see Fig. 27 for examples). Furthermore, two domains may have a lower density of mismatches if their interface is in one of the three chain directions rather than another (see Fig. 28 for an example of two such domains). This is very different from the situation we en-

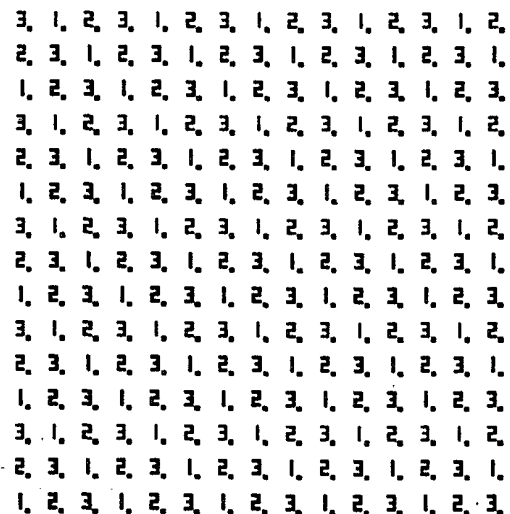


FIG. 25. A configuration with ordered spins and constraints. All the spins are down and the constraints are as shown.

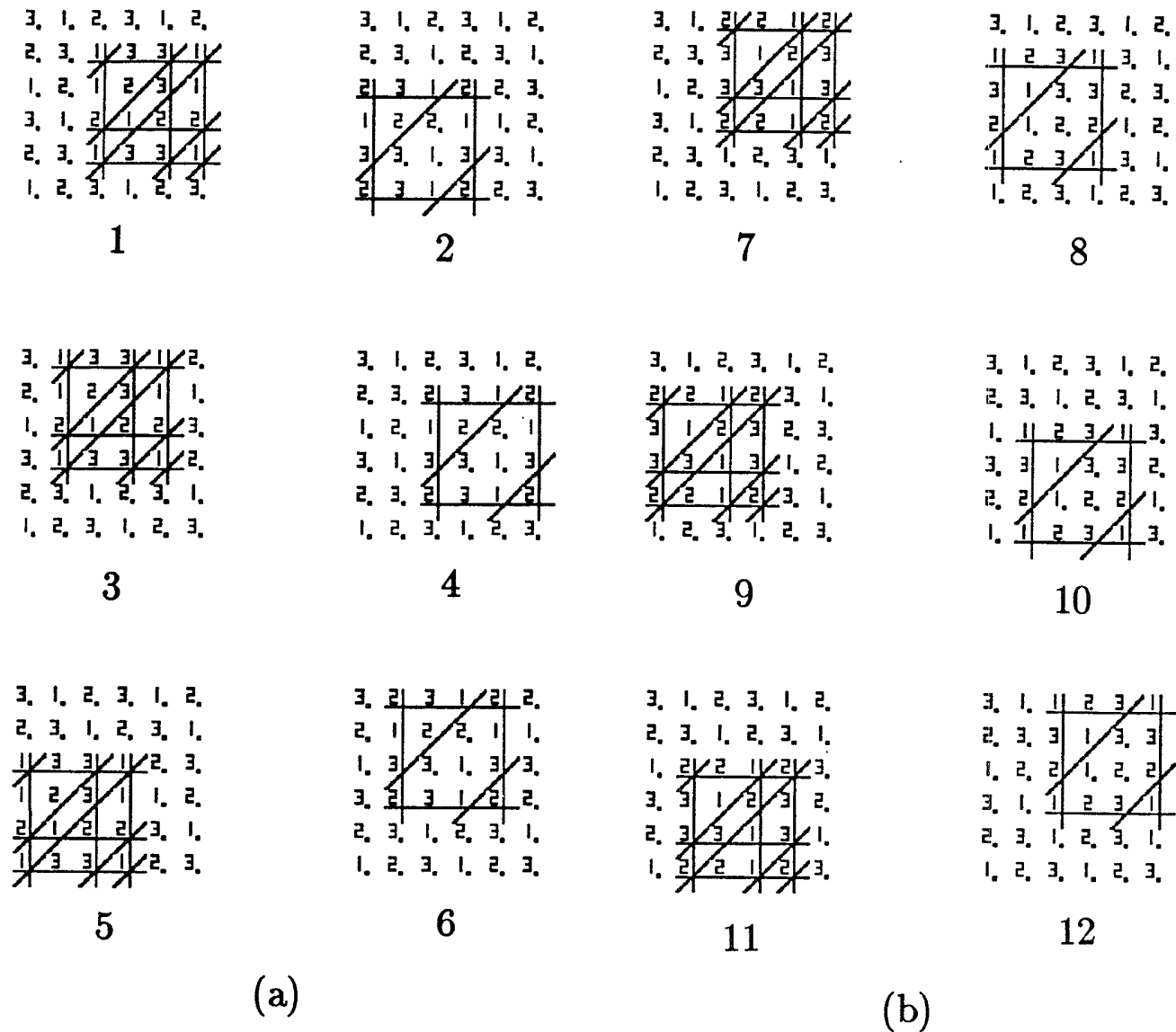


FIG. 26. Twelve of the 14 ground-state configurations for the case of ordered constraints (the two not shown have all spins up and all spins down) are as depicted in (a) and (b). The three spin configurations in each column are related by translations; the two configurations in the same row are negatives of each other. Although the ground-state configurations have 3×3 periodicity, we have instead shown a 4×4 portion since this makes it easier to identify the different ground states. In each case this 4×4 lattice is embedded in the initial spin and constraint configuration shown in Fig. 25.

countered in the previous case where the initialization was given by ordered spins and random constraints. In that case, the two ground states were negatives of each other, and had a mismatch density of six regardless of the direction of the boundary between them. We will discuss later the possible implications of this difference for the relaxation process.

Since the system with ordered constraints has 14 ground states rather than two, we expect on general grounds that it will relax more slowly than the system with random constraints discussed in the preceding section. The competition between these many degenerate states will make it difficult for the system to sort itself out

into a single phase. After being quenched from a high temperature, the system will initially contain a large number of domains of many different ground states that are small compared to the size of the system. Any given domain will be bordered by several other domains. In a system with only two ground states, roughly half of the neighboring domains will be of the same phase as the given domain, allowing it to grow by merger. In this way, small domains of one phase will coalesce to form larger domains. In a system with 14 ground states, it is improbable that the neighboring domains will be of the same phase—making it much less likely that a domain will grow by merging with neighboring domains.

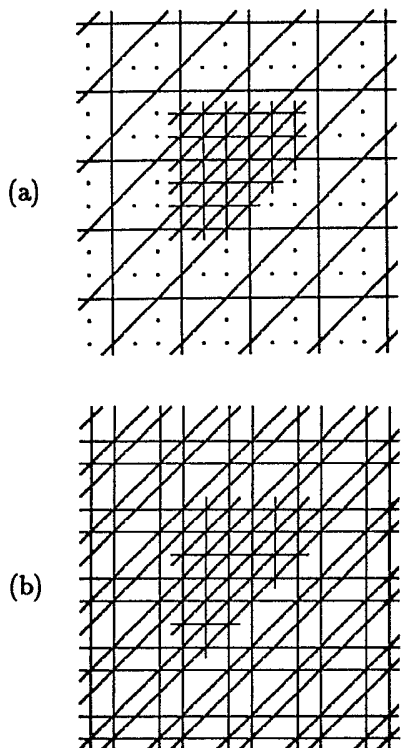


FIG. 27. (a) A domain of all up spins surrounded by another ground-state configuration (No. 6 in Fig. 26). The domain of up spins is shaped so that the boundary orientations include the \hat{x} , \hat{y} , and $\hat{x}+\hat{y}$ directions. In this case, the boundary has four spin mismatches per three lattice sites. (b) The same domain of all up spins surrounded by a different ground-state configuration than that in (a) (No. 11 in Fig. 26). In this case, the boundary has two spin mismatches per three lattice sites.

There is some evidence that when the number of ground states exceeds the dimensionality of the system, the relaxation may change in a qualitative manner. Lifshitz¹⁷ was the first to suggest that the growth of domains may be limited in systems where the number of ground states p is given by $p \geq d+1$, where d is the dimensionality of the system. He argues that minimizing the boundary energy at the junction of $d+1$ domains fixes the orientation of the boundaries. Since changing the orientation of the boundaries costs energy, this gives rise to a locally stable domain structure, making it difficult to relax to the zero-energy ground state. Safran¹⁸ later suggested that domain sizes equilibrate as a power law in time for $p < d+1$ and as a logarithmic function of time for $p \geq d+1$. However, more recent work by Safran and co-workers¹⁹⁻²¹ suggests that the situation is somewhat more complicated. When $p \geq d+1$, configurations of domains may occur within some models that are pinned at low temperatures since any variation of the domain walls costs energy. If such configurations occur frequently enough throughout a system, domain growth will be extremely slow. As the temperature is increased, such configurations will become unpinned. The occurrence of such pinning depends on the details of the model and is not universal.

We now consider the effects of boundary energies on

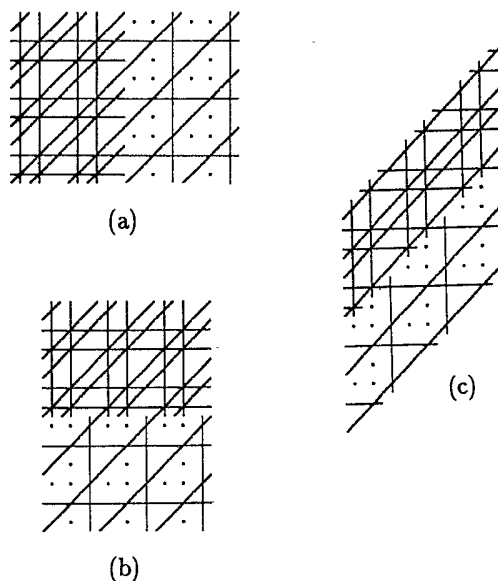


FIG. 28. (a) Two domains of different ground-state configurations (given by Nos. 4 and 11 in Fig. 26) shown with their boundary in the \hat{y} direction. In this case there are two mismatches per three lattice sites of boundary—one in the \hat{x} direction and one in the $\hat{x}+\hat{y}$ direction. (b) The same two domains with the boundary in the \hat{x} direction. In this case there are four mismatches per three lattice sites of boundary—three in the \hat{x} direction and one in the $\hat{x}+\hat{y}$ direction. (c) The same two domains with the boundary in the $\hat{x}+\hat{y}$ direction. In this case there are also four mismatches per three lattice sites of boundary—three in the \hat{x} direction and one in the \hat{y} direction.

domain growth in our system. Since some neighboring domains prefer an interface oriented in a specific direction, it will be possible to form patterns of four (or more) domains such that shrinking any of the four will result in a higher mismatch density locally, thus inhibiting the relaxation to one of the ground states. (See Fig. 29 for an example of a domain structure with four domains that is

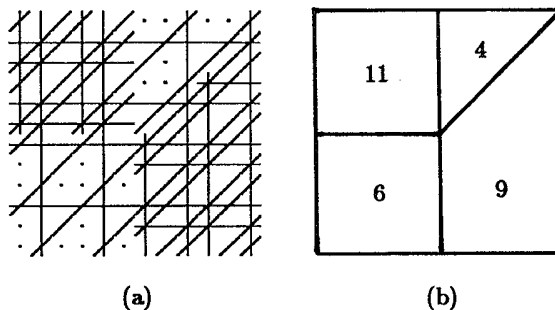


FIG. 29. (a) An example of a domain structure where the boundaries are in their preferred orientation. For each boundary, the mismatch density is two. Shrinking or expanding one of the four domains distorts the boundaries and creates additional spin mismatches, thus inhibiting the structure from relaxing to a single ground-state configuration. (b) A schematic drawing of the domain structure in (a), where the numbers refer to the labeling of the different ground-state configurations in Fig. 26.

locally stable.) However, such locally stable configurations will not occur in general, since not all pairs of domains have a preferred boundary direction.

Another consideration is that when a domain that is bounded by more than one other phase shrinks, the length of the boundary between two of its neighboring domains will increase (see Fig. 30). Since some pairs of domains are better matched than others, shrinking a domain may result in a greater number of spin mismatches locally. This will be the case if the boundaries that are increased in length have a higher mismatch density than the boundaries that are decreased in the process of shrinking a domain (again, see Fig. 30).

Thus, it seems plausible that the effect of different mismatch densities for different domain pairs and for different orientations of domain boundaries will be to slow the relaxation process. However, we are not able to predict how dramatic this effect will be for our system.

In order to compare the relaxation process of this system initialized with ordered spins and ordered constraints (which we will refer to as "ordered-ordered") with that of the two-ground-state system given by an initialization with ordered spins and random constraints ("ordered-random"), we can plot the number of spin mismatches as a function of time for both systems. However, the average boundary energy differs in the two cases—for the ordered-random initialization, since the two ground states are negatives of each other, the boundary energy is always six mismatches per three lattice constants of boundary; for the ordered-ordered initialization the average boundary energy is observed to be between two and three. Thus, comparing the number of mismatches in the two systems does not give an accurate measure of the relative lengths of the domain boundaries or of the relative sizes of the domains. In comparing the two systems, the size of the domains will be a better measure of how far the system is from the ground state than the number of spin mismatches. It is therefore necessary to examine the spin configurations along with the mismatch curves.

The number of spin mismatches is graphed as a func-

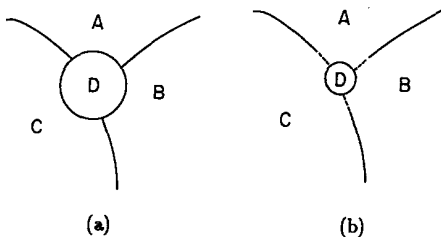


FIG. 30. (a) A domain structure with four domains. (b) Domain *D* has shrunk, thus decreasing the lengths of the *AB*, *BD*, and *DC* boundaries and increasing the lengths of the *AB*, *BC*, and *AC* boundaries (as indicated by the dotted lines). If the mismatch density for boundaries *AB*, *BC*, and *AC* is high compared to that of boundaries *AD*, *BD*, and *CD* then the configuration in (b) will have a greater number of spin mismatches than that in (a). If this is the case, it will not be energetically favorable for domain *D* to shrink.

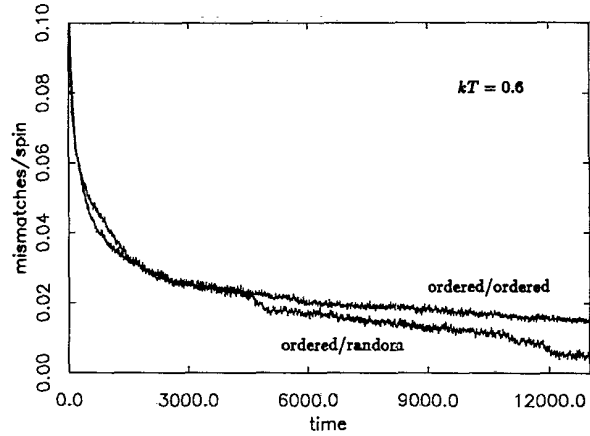


FIG. 31. The number of spin mismatches as a function of the number of time steps for a quench to $kT = 0.6$ for the ordered-random configuration of Fig. 24 and the ordered-ordered configuration of Fig. 32. After 12000 time steps, the ordered-random system has relaxed to its equilibrium mismatch density.

tion of time in Fig. 31 for an ordered-ordered system that has been quenched to a temperature of $kT = 0.6$, along with the comparable curve for the ordered-random system from Fig. 20. By 5000 time steps, the ordered-random system contains a single isolated domain; the majority domains at that time has grown to the size of the system. In examining the spin configuration for the ordered-ordered system after a comparable number of time steps [Figs. 32(a)–32(d)], we find that this system contains numerous smaller domains. This domain structure changes very slowly, as is evident from Figs. 32 and 33. After 12000 time steps the ordered-random system has relaxed to its equilibrium mismatch density, but the ordered-ordered system still contains numerous domains and is relaxing very slowly.

From the results discussed above, it seems clear that the ordered-ordered system with 14 ground states relaxes much more slowly than the ordered-random system with two ground states. We are unable, however, to say whether the relaxation is qualitatively different (as in the models of Safran and co-workers^{19,21}) or whether the functional form of the time dependence of domain growth is the same in both cases.

3. Random spins and random constraints

A system initialized with randomly assigned spins and constraints in general has no accessible ground states. The lowest-energy configuration for such a system therefore has a nonzero number of spin mismatches.

We consider the possibility that this system will exhibit glassy behavior, and compare its relaxation to that of the ordered-random system upon cooling. For the ordered-random system, we randomize the spins at high temperature ($kT = 1000$), cool the system rapidly to $kT = 10$, and then cool exponentially from $kT = 10$ to $kT = 0.01$. We determine the cooling rate for which the system always relaxes to the ground state, implying that it remains in equilibrium upon cooling at this rate. For the random-random system we cool at the same rate for which the

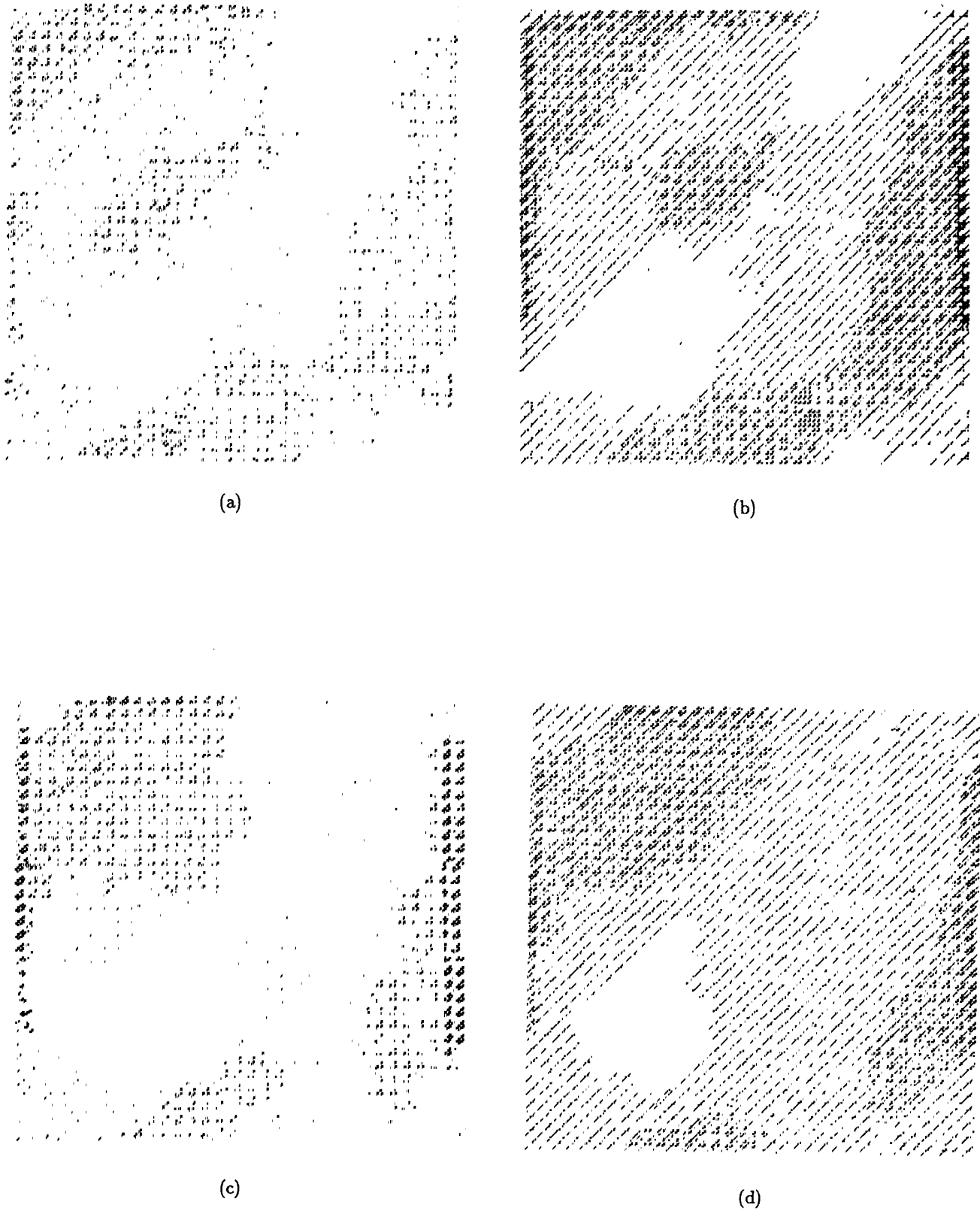


FIG. 32. (a) The spin configuration after 2000 time steps for an ordered-ordered system that has been quenched to $kT=0.6$. The spin mismatches for this system are graphed in Fig. 31. (b) The spin configuration after 4500 time steps. (c) The spin configuration after 8500 time steps. (d) The spin configuration after 11 000 time steps.

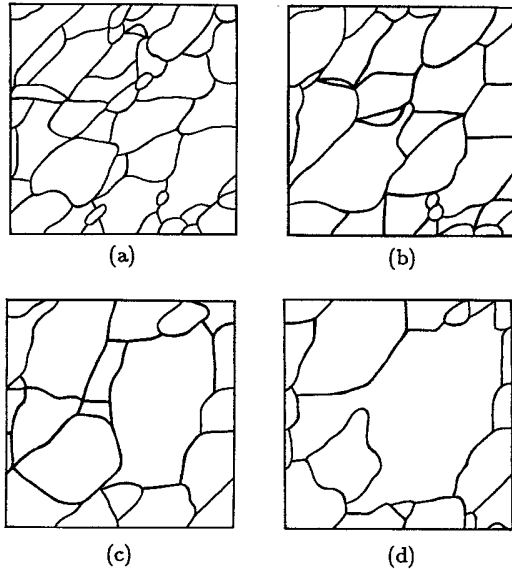


FIG. 33. The evolution of the domain structure of the system shown in Fig. 32. These figures correspond to Figs. 32(a)–32(d), and show the boundaries of the domains in those spin configurations.

ordered-random system remained in equilibrium.

We find that on repeated coolings from the same initial spin and constraint configuration, the random-random system relaxes to different spin configurations that are nearly degenerate in energy. The overlap of these configurations with each other can be calculated by summing the products of the corresponding spins of two configurations, and dividing by the total number of spins. This calculation gives values on the order of 0.1 for the overlap of several configurations produced in this way. (The overlap between two completely random configurations should be approximately 0.02; correlations between spins in a system would increase this value.) Furthermore, one can verify that these configurations are relatively stable by calculating the overlap between each configuration and itself 1000 time steps later. In each case, this overlap is approximately 0.9.

The presence of a large number of nearly degenerate minima corresponding to different final states is characteristic of systems exhibiting glassy behavior. Thus, we expect the dynamics of this system to be extremely slow.

IV. IMPLICATIONS FOR PHASON RELAXATION IN QUASICRYSTALS

In our investigations of the spin model, we find that two features have the effect of slowing the dynamics of relaxation: (1) the existence of constraints on the motion of mismatches, and (2) the existence of a large number of ground states. In this final section, we discuss the implications of these results for phason dynamics in the Penrose tiling and in laboratory quasicrystals.

A. The Penrose tiling

The constraints on spin flips in our model slow the relaxation of the system, especially at low temperatures where the probability of creating a pair of mismatches is very small. At these temperatures the system is essentially frozen. These results suggest that the constraints on worm flips in the Penrose tiling will also slow the relaxation of phason strain in that system. In fact, we would expect this effect to be more pronounced in the Penrose tiling: in the spin model, only one spin needs to flip in order to free a constrained spin, whereas in the Penrose tiling two worms may have to flip in order to free a constrained worm.

We also find in the spin model that the number of ground states of the system is an important parameter for understanding the rate of relaxation. Below, we first describe how ground-state domains can be defined in a Penrose tiling, and then discuss the implications of the results of our spin model for phason relaxation in the Penrose tiling.

An infinite Penrose tiling has an infinite number of ground states, with the different ground states corresponding to different elements of the Penrose LI class. As discussed previously, elements of this class differ from one another by uniform shifts of the phason field \mathbf{w} . Thus, two Penrose tilings corresponding to different ground-state configurations will differ only by flips of infinite worms, with the density of such worm flips proportional to the difference in the values of \mathbf{w} in the two tilings. Beginning with a tiling that has a uniform phason field \mathbf{w}_1 , we can construct a domain with phason field \mathbf{w}_2 within a region R by considering the set of infinite worms intersecting R that flip in the tiling as \mathbf{w} is changed from \mathbf{w}_1 to \mathbf{w}_2 , and flipping only the sections of those worms that lie within R . This procedure will result in mismatches along the boundary of R , giving rise to a boundary energy between the two domains. The number of worms within R that have been flipped relative to the surrounding tiling, and thus the boundary energy, will be proportional to the difference in \mathbf{w} between the two domains. Notice that this procedure does not lead to mismatches at all points along the boundary of R ; some sets of tiles will be compatible with the structure of both domains. This is analogous to the ordered-ordered system in our spin model, where some chains have no mismatches as they pass from one domain into another.

As an aside, we note that as in the spin model, any isolated domain of one phase (corresponding to \mathbf{w}_2) surrounded by a second phase (corresponding to \mathbf{w}_1) can shrink to zero size at zero temperature (see Fig. 15). This follows from our prescription for constructing domains by changing \mathbf{w} continuously from \mathbf{w}_1 to \mathbf{w}_2 and flipping the corresponding worm segments lying within the domain. Since these flips occur in a definite sequence, the domain can be removed by undoing this set of flips in the reverse order. Since creating the domain did not require producing mismatches in the interior of the domain, neither will reversing the process.

How, then, does the existence of an infinite number of ground states affect the phason relaxation in the Penrose

tiling? In our spin model, the presence of numerous ground states in the ordered-ordered system resulted in very slow relaxation. As we discussed in that case, one expects on general grounds that a system with numerous ground states will relax very slowly even at high temperatures: domain growth will be inhibited because it is unlikely that domains of one phase will lie near each other and be able to coalesce to form a larger domain. However, the existence of an infinite rather than a finite number of ground states in the Penrose tiling is a potentially important difference that we now discuss.

In both our spin model and the Penrose tiling, the phason strain is manifested in terms of mismatches that are discrete defects. The total energy cost of these defects is simply given by the sum of the energy cost of the individual defects. In terms of the phason field \mathbf{w} , such an energy density has the form $\nabla \mathbf{w}$.

For our spin model, which has a finite number of ground states, a configuration that initially has a random distribution of defects will relax to a state where local regions are in one of the ground-state configurations. Thus, as we observe, the system will contain well-defined domains with spin mismatches on the boundaries between domains. We can describe this system by a nonuniform phase field \mathbf{w} . Consider a case where the phason field takes on the value \mathbf{w}_1 (corresponding to one ground-state configuration) in the neighborhood of \mathbf{r}_1 and the value \mathbf{w}_2 (corresponding to a second ground-state configuration) in the neighborhood of \mathbf{r}_2 . How does \mathbf{w} vary between those two points? At low temperatures, where entropy effects are minimal, the phason field will jump sharply from \mathbf{w}_1 to \mathbf{w}_2 somewhere between \mathbf{r}_1 and \mathbf{r}_2 , thereby maximizing the area that is in a ground state. At nonzero temperatures, entropy considerations will favor mismatches that are more dispersed, corresponding to broadened domain walls. Domain wall broadening is consistent with a free-energy contribution that is proportional to $(\nabla \mathbf{w})^2$.

In a system with an infinite number of ground states, such as the Penrose tiling, it is possible for the phason field \mathbf{w} to vary smoothly between the two points \mathbf{r}_1 and \mathbf{r}_2 with the system being in a ground state at all points in between, since there are an infinite number of ground states with a value of \mathbf{w} between \mathbf{w}_1 and \mathbf{w}_2 . (Something analogous can also happen in our spin model: the system can interpolate between \mathbf{w}_1 and \mathbf{w}_2 by inserting one or more ground-state domains with a value of \mathbf{w} that lies between \mathbf{w}_1 and \mathbf{w}_2 .) In the Penrose tiling, it is thus possible for the domain walls to spread out so that there are no identifiable domains. By interpolating between ground states in this way, the entropy can be maximized. In this case, we would expect the phason dynamics to be given by a hydrodynamic description. The existence of an infinite number of ground states, however, does not necessarily result in a slowly varying phason field: sharp domain walls can result if there is an effective attraction between defects. For example, in a crystal, dislocation lines attract and a distorted crystal will tend to form crystal domains separated by rows of dislocation lines.

If the defects in the Penrose tiling are made to attract via a potential that includes interaction between nearest-

neighbor tiles, then a Penrose tiling with phason strain may consist of domains of different ground-state configurations separated by sharp walls. We expect that this will give rise to a slow relaxation rate even at high temperatures, as in the ordered-ordered spin system. In fact, this effect may be more pronounced in the Penrose tiling because the probability that a domain of a given phase will be in the vicinity of another domain of the same phase scales with the number of ground states, p , as z/p , where z is the number of neighboring domains.

Whether the presence of such domains merely stretches the time scale of the relaxation (with the correlation length growing as a power law, as is found for many systems, including the two-dimensional Ising model) or whether it changes the time dependence of the relaxation process (with the correlation length growing only logarithmically with time) remains an open question that requires further study. As discussed earlier, there are indications that logarithmically slow relaxation can arise for some geometries when the number of ground states is equal to or greater than the dimensionality of the system.^{17,18} Recent simulations find that this logarithmic behavior depends critically on the geometry of the lattice of the system, with some geometries leading to domain structures that are effectively pinned.^{19,21} Whether this is true for the unusual fivefold quasiperiodic geometry found in the Penrose tiling remains an open question.

B. Laboratory quasicrystals

The same analysis discussed for the Penrose tiling also applies to laboratory quasicrystals. If the energetics of phason strain in quasicrystals leads to narrow domain walls, then the slow dynamics found in our model may be applicable to real systems. (This could be the case even if our results were not applicable to the Penrose tiling.) On the other hand, the most energetically favorable configuration may be to spread the phason strain over an extended region, so that the more appropriate description of quasicrystals would be given by a continuum elastic theory. One would not expect the dynamics of such a system to be those found in the spin model.

The discovery of quasicrystals with sharp Bragg peaks may indicate that the constraints on phason relaxation are not universal but depend, for example, on structural differences between systems. Those quasicrystals displaying sharp peaks have a "body-centered cubic" reciprocal lattice, rather than the "simple cubic" lattice exhibited by all other quasicrystals that have been studied.⁴

We note two additional points. Since phasons correspond to local rearrangements of atoms, in general one expects large energy barriers to such motion, with time scales on the order of those for vacancy diffusion in crystals. Since such processes are thermally activated, they occur much less frequently at low temperatures. In our model, this diffusion rate corresponds to the attempt rate for flipping spins (or hexagons in the Penrose tiling) and is taken to be unity. Thus, the time scale in our model is given by the inverse of the diffusion rate, and can become very long compared to laboratory time scales, especially at low temperatures.

And finally, in real materials exhibiting quasicrystalline order, we expect that the growth process will introduce defects other than just phason strain, such as dislocations. A quasicrystal with dislocations frozen in will not be able to relax to a perfectly ordered quasicrystal. Thus, a laboratory quasicrystal may not be able to reach a ground-state configuration at all, and in that case the more appropriate spin model may be that given by randomly assigned spins and constraints. The evidence we found that the random-random system exhibits glassy be-

havior may indicate that the disorder in the phason field will be frozen in by glassy dynamics in a quasicrystal with defects other than just phason strain.

ACKNOWLEDGMENTS

We would like to thank David Divincenzo, Joshua Socolar, and Peter Bancel for helpful discussions. This work was partially supported by NSF Grant Nos. DMR86-13368 and DMR85-03544.

*Current address: Center for International Security Studies, School of Public Affairs, University of Maryland, Suite 400, 7100 Baltimore Blvd., College Park, MD 20740.

†Current address: Federation of American Scientists, 307 Massachusetts Ave., NE, Washington, D.C. 20002.

‡Current address: Department of Physics, University of California, Berkeley, California 94720.

¹D. Shechtman, I. Blech, D. Gratias, and J. W. Cahn, *Phys. Rev. Lett.* **53**, 1951 (1984); Dov Levine and P. J. Steinhardt, *ibid.* **53**, 2477 (1984).

²P. Bak, *Phys. Rev. Lett.* **54**, 1517 (1985).

³D. Levine, T. C. Lubensky, S. Ostlund, S. Ramaswamy, P. J. Steinhardt, and John Toner, *Phys. Rev. Lett.* **54**, 1520 (1985).

⁴A. P. Tsai, A. Inoue, and T. Masumoto, *Jpn. J. Appl. Phys.* **26**, L1505 (1987); S. Ebalard and F. Spaepen, *J. Mat. Res.* **4**, 39 (1988); C. A. Guryan, A. I. Goldman, P. W. Stephens, K. Hiraga, A. P. Tsai, A. Inoue, and T. Masumoto, *Phys. Rev. Lett.* **62**, 2409 (1989); P. A. Bancel, *ibid.* **63**, 2741 (1989).

⁵T. C. Lubensky, J. E. S. Socolar, P. J. Steinhardt, P. A. Bancel, and P. A. Heiney, *Phys. Rev. Lett.* **57**, 1440 (1986).

⁶P. M. Horn, W. Malzfeldt, D. P. DiVincenzo, J. Toner, and R. Gambino, *Phys. Rev. Lett.* **57**, 1444 (1986).

⁷P. A. Heiney, P. A. Bancel, P. M. Horn, J. L. Jordan, S. Laplaca, J. Angilello, and F. W. Gayle, *Science* **238**, 660 (1987).

⁸R. Penrose, *Bull. Inst. Math. Appl.* **10**, 266 (1974).

⁹M. Gardner, *Sci. Am.* **236** (1), 110 (1977).

¹⁰J. E. S. Socolar, T. C. Lubensky, and P. J. Steinhardt, *Phys. Rev. B* **34**, 3345 (1986).

¹¹J. E. S. Socolar, *J. Phys. (Paris Colloq.)* **47**, C3-217 (1986).

¹²G. H. Fredrickson and H. C. Anderson, *Phys. Rev. Lett.* **53**, 1244 (1984); G. H. Fredrickson and S. A. Brawer, *J. Chem. Phys.* **84**, 3351 (1986).

¹³D. Levine and P. J. Steinhardt, *Phys. Rev. B* **34**, 596 (1986).

¹⁴J. E. S. Socolar and P. J. Steinhardt, *Phys. Rev. B* **34**, 617 (1986).

¹⁵We have also studied analogous models with two spins per site, whose behavior was not as interesting: Lisbeth D. Gronlund, Doctoral thesis, Cornell University, 1988 (unpublished).

¹⁶R. J. Glauber, *J. Math. Phys.* **4**, 294 (1963).

¹⁷I. M. Lifshitz, *Zh. Eksp. Teor. Fiz.* **42**, 1354 (1962) [*Soviet Physics JETP* **15**, 939 (1962)].

¹⁸S. A. Safran, *Phys. Rev. Lett.* **46**, 1581 (1981).

¹⁹S. A. Safran, P. S. Sahni, and G. S. Grest, *Phys. Rev. B* **28**, 2693 (1983).

²⁰P. S. Sahni, G. S. Grest, and S. A. Safran, *Phys. Rev. Lett.* **50**, 60 (1983).

²¹P. S. Sahni, D. J. Srolovitz, G. S. Grest, M. P. Anderson, and S. A. Safran, *Phys. Rev. B* **28**, 2705 (1983).